Modeling the manipulator and flipper pose effects on tip over stability of a tracked mobile manipulator

Chioniso Dube
Mobile Intelligent Autonomous Systems
Council for Scientific and Industrial Research,
South Africa
Email: cdube@csir.co.za

***Abstract*—Mobile manipulators are used in a number of different applications such as bomb disposal, mining robotics, and search and rescue operations. These mobile manipulators are highly susceptible to tip over due to the motion of the manipulator or the gradient of the slope being traversed by the platform. This paper presents the model of a tracked mobile manipulator for tip-over stability analysis in stope mining environments. The Force Angle stability measure is used to compute the stability index of the platform. An environment is simulated using a gradient vector field and a simulated iRobot PackBot platform is modeled moving through the environment. The PackBot manipulator motion is modeled using the forward kinematics of serial structured manipulators. Action of the flippers has the effect of changing the tip over axis and stability index of the platform. The geometry of the platform is used to compute the resultant tip over axis given the angle of the flippers. The overall stability based on the slope of the environment, the manipulator pose and the flipper angle is then computed. The results give new insight into tip over prevention for tracked mobile manipulators.**

I. Introduction

Mobile manipulators are robotic platforms consisting of a robotic manipulator mounted on a tracked, legged or wheeled base and are used in a number of different applications such as mining robotics, bomb disposal, and search and rescue operations. Such mobile manipulators are highly susceptible to tip over due to the motion of the manipulator or the gradient of the slope being traversed by the platform. This paper presents the model of a tracked mobile manipulator for tip-over stability analysis. (See figure 1)

Fig. 1. PackBot 510 [12]

A number of stability measures and algorithms have been developed by various researchers to assess the stability of a robot and predict tip over conditions. They include the Zero-Moment Point (ZMP), Force-Angle stability measure (FA), and Moment-Height Stability measure (MHS). The Zero-Moment Point is a point on the ground where the sum of all the forces and moments acting on the robot platform can be replaced by a single force [1]. It was originally derived for stability analysis of bipedal robots, and it has been adapted to other types of mobile robots [1], [2]. A different approach to stability analysis was proposed by Papadopoulos and Rey [3], [4], which they termed the Force-Angle stability measure (FA). The FA algorithm measures the angle of the total applied force on the center of mass of the platform with reference to the support polygon, which is derived from the ground contact points of the robot [5]. Papadopolus and Rey derive two measures, the static FA which takes into account the forces due to the wieght of the manipulator and base platform and the dynamic FA which takes into account effects of the forces generated be the motion of the manipulator. Due to the complexity of computing dyanamics of a multi degree of freedom manipulator, in their simulation, they simplify the dynamics model of the manipulator in order to obtain the dynamic FA measure [4]. They find that both the dynamic and static measures predict tip over at the same point in time [4]. Similar to the FA measure, Moosavian and Alipour proposed the Moment-Height Stability measure [6] with also accounts for the robot's inertia about each axis of the support polygon and scales results by the height of the robot's center of mass.

Tip-over stability alogorythms have been compared by Moosavian and Alipour in [7] using simulated data. They found that some measures were too confident or too restrictive as compared to others. Roan et al [8] compare the ZMP, FA, MHS using a modified PackBot Fido from iRobot. The mobile robot platform was dynamically modeled in software, and the ZMP, FA, and MHS algorithms were coded. The robot was then fitted with an inertial measurement (IMU) based data collection system and driven over various obstacles and the data used to calculate the tipover measures over time [8]. Roan et al results show that the FA and MHS had very similar performance and performed better than the ZMP. In their test, the flipper and manipulator are kept at a single position and so the results do not take into consideration their effects on the stability of the platform.

This paper models and investigates the effects of the manipulator and flipper pose on the stability of a tracked mobile manipulator, the PackBot from iRobot. The PackBot has a manipulator with a 4 DOF arm and a 2 DOF camera and two flippers at the front of the platform as shown in figure 1. The static Force Angle stability measure formulated by [3], [5] is used here to compute the stability index of the platform. A model of the PackBot in relation to the flipper state of contact with the ground is developed. The tip over stability based on the flipper and manipulator pose is then analysed.

II. The Force Angle Stability Measure [5]

The FA measure as described in [5], is used in this study and is summarised in this section.

A. Planar Example

The planar example of the FA measure is shown in Figure 2. The system has two contact points and a system Center of Mass (C.M.) which is subject to a net force $\boldsymbol{f_r}$. The net force $\boldsymbol{f_r}$ is the sum of all forces acting on the system excluding the support reaction forces which do not contribute to tipover instability. This net force vector subtends two angles, θ_1 and θ_2, with the two tipover axis normals $\boldsymbol{l_1}$ and $\boldsymbol{l_2}$, and is at a distance of $\|\boldsymbol{d_1}\|$ and $\|\boldsymbol{d_2}\|$ respectively from the tipover axes. The Force-Angle stability measure, β, is the minimum of the product of θ_i , $\|\boldsymbol{d_i}\|$, and $\|\boldsymbol{f_r}\|$. [5]

Thus the FA measure is [5]:

$$\beta = min\left(\theta_i \cdot \|\boldsymbol{d_i}\| \cdot \|\boldsymbol{f_r}\|\right)$$

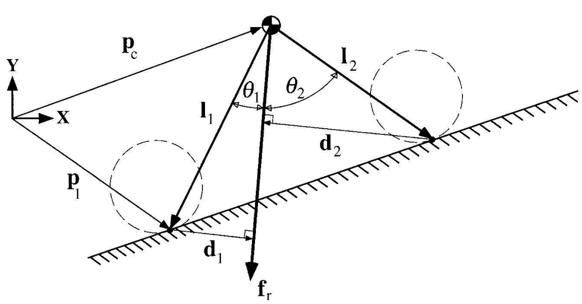

Fig. 2. Force Angle Stability Measure - Planar [5]

Tip over instability occurs when β approaches zero. The angle θ_i captures the effect of changes in the system C.M. height along the net force vector $\boldsymbol{f_r}$ and the distance $\|\boldsymbol{d_i}\|$ captures the effect of changes in the moment contribution of the net force. Weighing by the magnitude of $\boldsymbol{f_r}$ captures effects of total weight of the system since the disturdance force required to tip the vehicle becomes smaller as the magnitude of $\boldsymbol{f_r}$ decreases. [5]

B. General Form

For the general case, $\boldsymbol{p_i}$ represents the location of a ground contact point of the platform [5]:

$$\boldsymbol{p_i} = [p_x, p_y, p_z]_i^T$$

and $\boldsymbol{p_c}$ represents the location of the system C.M. [5]:

$$\boldsymbol{p_c} = \frac{\sum_j \boldsymbol{p_{mass_j}} m_j}{m_{tot}}$$

where $i = \{1, \ldots, n-1\}$ and $\boldsymbol{p_{mass_j}}$ is the location of the mass of the jth member of the system and m_{tot} is the total system mass. [5]

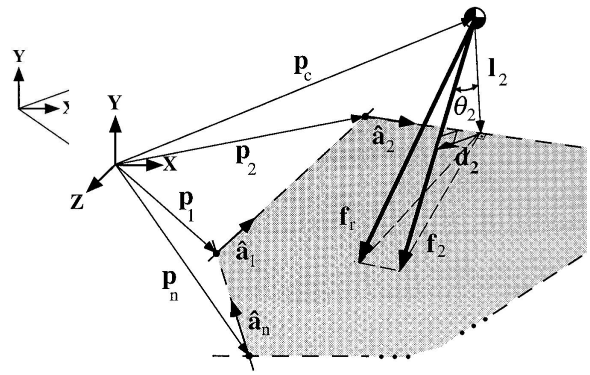

Fig. 3. Force Angle Stability Measure - 3d [5]

The lines which join the ground contact points are the candidate tipover mode axes, $\boldsymbol{a_i}$. [5]

$$\boldsymbol{a_i} = \boldsymbol{p_{i+1}} - \boldsymbol{p_i}$$

$$\boldsymbol{a_n} = \boldsymbol{p_l} - \boldsymbol{p_n}$$

$$\boldsymbol{\hat{a}_i} = \frac{\boldsymbol{a}}{\|\boldsymbol{a}\|}$$

The tipover axis normals l_i which pass through the system C.M. are [5]:

$$l_i = \left(\boldsymbol{I} - \boldsymbol{\hat{a}_i}\boldsymbol{\hat{a}_i^T}\right)\left(\boldsymbol{p_{i+1}} - \boldsymbol{p_c}\right)$$

where $\boldsymbol{I}$ is the 3×3 identity matrix.

The component of the force acting about each tip over axis is [5]:

$$\boldsymbol{f_i} = \left(\boldsymbol{I} - \boldsymbol{\hat{a}_i}\boldsymbol{\hat{a}_i^T}\right)\boldsymbol{f_r}$$

and the moment component is [5]:

$$\boldsymbol{n_i} = \left(\boldsymbol{\hat{a}_i}\boldsymbol{\hat{a}_i^T}\right)\boldsymbol{n_r}$$

The effective net force vector is [5]:

$$\boldsymbol{f_i^*} = \boldsymbol{f_i} + \frac{\boldsymbol{\hat{l}_i} \times \boldsymbol{n_i}}{\left\|\boldsymbol{\hat{l}_i}\right\|}$$

The distance of the force from the tip over axes is [5]:

$$\boldsymbol{d_i} = -\boldsymbol{l_i} + \left(\boldsymbol{l_i^T} \cdot \boldsymbol{\hat{f}_i^*}\right)\boldsymbol{\hat{f}_i^*}$$

The angle of the force from the tip over axes is [5]:

$$\theta_i = \sigma_i \cos^{-1}\left(\hat{\boldsymbol{l}}_{\boldsymbol{i}} \cdot \hat{\boldsymbol{f}}_{\boldsymbol{i}}^{*}\right)$$

where [5]:

$$0 \leq \frac{\theta_i}{\sigma_i} \leq \pi$$

and [5]:

$$\sigma_i = \begin{cases} +1 & \left(\hat{\boldsymbol{f}}_{\boldsymbol{i}}^{*} \times \hat{\boldsymbol{l}}_{\boldsymbol{i}}\right) \cdot \hat{\boldsymbol{a}} \\ -1 & otherwise \end{cases}$$

III. Modelling the PackBot

The modelling of the PackBot manipulator and flipper pose is described in this section.

A. Flippers

Flippers can either be up or in contact with the ground as shown in figure 4. The minimum and maximum angles, ϕ_{min} and ϕ_{max}, for which the flippers will be in contact with the ground are found as follows:

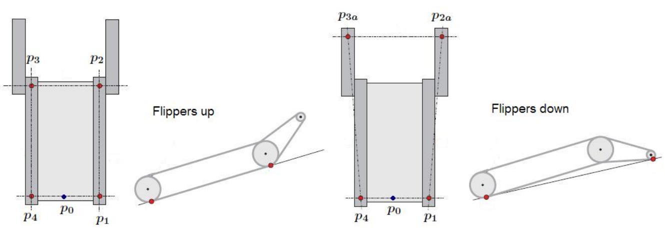

Fig. 4. Flipper positions

$$\phi_{min} = \arcsin\left(\frac{H_{pb} - R_f}{L_f}\right)$$

$$\phi_{max} = 180 - \phi_{min}$$

where the PackBot dimensions are:
L_{pb} is the length of the base,
W_{pb} is the width of the base,
H_{pb} is the height of the base.

1) Flippers up: The flippers are up when the flipper angle ϕ_f is outside the range of ϕ_{min} and ϕ_{max} i.e. $\sin(\phi_f) > \sin(\phi_{min})$. Given the position of the PackBot $\boldsymbol{p_0}$, (here it is assumed the position is measured at the center of the rear axis of the PackBot), the slope vector $\boldsymbol{s_p}$ and normal of the slope $\boldsymbol{n_p}$ and the front of the PackBot $\boldsymbol{w_p}$, the contact points are:

$$\boldsymbol{p_1} = \boldsymbol{p_0} - \boldsymbol{w_p} \times \frac{W_{pb}}{2}$$

$$\boldsymbol{p_2} = \boldsymbol{p_1} + \boldsymbol{s_p} \times L_{pb}$$

$$\boldsymbol{p_3} = \boldsymbol{p_2} + \boldsymbol{w_p} \times W_{pb}$$

$$\boldsymbol{p_4} = \boldsymbol{p_3} - \boldsymbol{s_p} \times L_{pb}$$

The vector and normal of the PackBot base is:

$$\boldsymbol{s_{pb}} = \boldsymbol{s_p}$$

$$\boldsymbol{n_{pb}} = \boldsymbol{n_p}$$

2) Flippers down: Once the flippers are in contact with the ground, ie if $\sin(\phi_f) \leq \sin(\phi_{min})$, the flipper motion changes the configuration of the PackBot. To calculate the configuration based on the flipper down angle, the contact points become, given the slope and normal of the slope and the front of the PackBot:

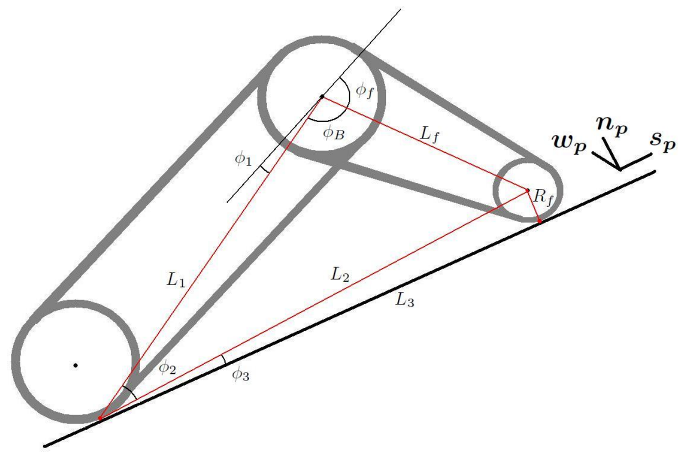

Fig. 5. Flipper Contact

$$\boldsymbol{p_{2a}} = \boldsymbol{p_1} + \boldsymbol{s_p} \times L_3$$

$$\boldsymbol{p_{3a}} = \boldsymbol{p_{2a}} + \boldsymbol{w_p} \times W_{pb}$$

$$\boldsymbol{p_2} = \boldsymbol{p_1} + \boldsymbol{s_p} \times L_{pb} \times \cos(\phi_2 + \phi_3 - \phi_1) + \boldsymbol{n_p} \times L_{pb} \times \sin(\phi_2 + \phi_3 - \phi_1)$$

where the lengths and angles as shown in figure 5 are:

$$L_3 = \sqrt{L_2^2 - R_f^2}$$

$$L_2 = \sqrt{L_1^2 + L_f^2 - 2L_1L_f\cos\phi_B}$$

$$L_1 = \sqrt{L_{pb}^2 + \left(\frac{H_{pb}}{2}\right)^2}$$

$$\phi_B = 180 - \phi_1 - \phi_f$$

$$\phi_1 = \arccos\left(\frac{L_{pb}}{L_1}\right)$$

$$\phi_2 = \arccos\left(\sqrt{\frac{L_1 + L_2 - L_f}{2L_1L_2}}\right)$$

$$\phi_3 = \arcsin\left(\frac{R_f}{L_2}\right)$$

The vector and normal of the PackBot base are:

$$\boldsymbol{s_{pb}} = \boldsymbol{s_p} \times \cos(\phi_2 + \phi_3 - \phi_1) + \boldsymbol{n_p} \times \sin(\phi_2 + \phi_3 - \phi_1)$$

$$\boldsymbol{n_{pb}} = \boldsymbol{s_{pb}} \times \boldsymbol{w_p}$$

B. Manipulator

Given the joint angles of the manipulator links, the position of the manipulator links are modelled using the forward kinematics of robot arms as described in [11]. From the forward kinematics, the location $\boldsymbol{q_j^*}$ of the jth link is obtained. Transforming the manipulator link postions from the PackBot coordinate frame to the enviroment frame:

$$\boldsymbol{q_j} = \boldsymbol{p_0} + \boldsymbol{s_{pb}} \times \boldsymbol{q_m} + \boldsymbol{n_{pb}} \times \boldsymbol{H_{pb}} + \boldsymbol{R} \times \boldsymbol{q_j^*}$$

where

$$\boldsymbol{R} = [\boldsymbol{w_p}, \boldsymbol{s_{pb}}, \boldsymbol{n_{pb}}]$$

$\boldsymbol{q_m}$ is the coordinate of the manipulator base in the PackBot frame

C. Center of mass

The PackBot system center of mass is affected by the manipulator center of mass and the base center of mass.

1) Center of mass of base: The center of mass position of the PackBot base is:

$$\boldsymbol{cm_b} = \boldsymbol{p_1} + \boldsymbol{s_{pb}} \times \frac{L_{pb}}{2} + \boldsymbol{w_{pb}} \times \frac{W_{pb}}{2} + \boldsymbol{n_{pb}} \times \frac{H_{pb}}{2}$$

2) Center of mass of manipulator: The center of mass of each link $\boldsymbol{cm_{qj}}$ is placed at the center of the link.

$$\boldsymbol{cm_m} = \frac{\sum_j \boldsymbol{cm_{qj}} \times m_{qj}}{m_m}$$

3) PackBot center of mass: The center of mass of the PackBot system is thus:

$$\boldsymbol{cm_{pb}} = \frac{\boldsymbol{cm_b} \times m_{pb} + \boldsymbol{cm_m} \times m_m}{m_b + m_m}$$

IV. RESULTS

The PackBot is simulated going through a range of motion on a range of different slopes. A slope angle below 0^o corresponds to the packBot facing downslope while above 0^o the PackBot faces upslope. The tip over stability index at each tip over axis is computed along with the overall tip over stability of the PackBot system. The index is normalised about the rest position of the PackBot, i.e. when the manipulator is stored and the flippers are up. A stability measure of 1 thus corresponds to the stability at the rest position.

Figure 6 shows the effect of the manipulator on tip over stability. The manipulator is modelled through two motions while keeping the flippers in the up position. For the first stage of motion, the center of mass of the manipulator is moved through a circle at a constant height above the PackBot base. For the second stage of motion, the center of mass of the maipulator is raised incremetally above the PackBot base. As seen in figure 6, there are two distinct regions of high stability as the center of mass of manipulator moves through the circle. The first region peaks when the manipulator is at 25^o (0^o corresponds to the manipulator rest position) and the second region peaks at 200^o. For the first region, the combined center of mass of the PackBot is kept near to the center of the Packbot base, making the system stable. The stability however decreases as the slope moves away from 0^o. The second region is only stable for slope angles below 0^o. At these slope angles, the robot is facing upslope and the weight of the manipulator is also upslope thus shifting the combined system center of mass upslope, which results in a more stable system. At slope angles above 0^o, the stability in the manipulator 200^o region rapidly decreases. This is because the robot is facing downslope and the weight of the manipulator is also downslope making the robot tip over about its front axis. Thus for slopes close to 0^o the manipulator should be kept close to 25^o and for slopes below 0^o the manipulator should be kept close to 200^o.

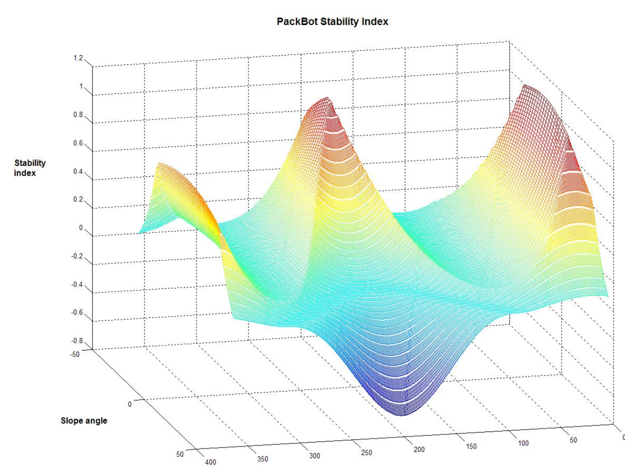

Fig. 6. Manipulator center of mass position effects on tip over stability

For the second stage of manipulator motion, the manipulator center of mass height is raised above the PackBot base. As seen in figure 7, there is a single plateaued stable region of manipulator height that changes in size with slope. Heights closer to the PackBot base are more stable. There is a small decrease in stability with height in the stable region. Thus at slope angles close to 0^o the center of mass height of the manipulator can be changed while ensuring stability. As slope angles move away from 0^o the stability of the system decreases rapidly at two distinct boundaries. As height increases, the range of slope angles for which the system would still be stable decreases. The PackBot is more unstable when facing downslope.

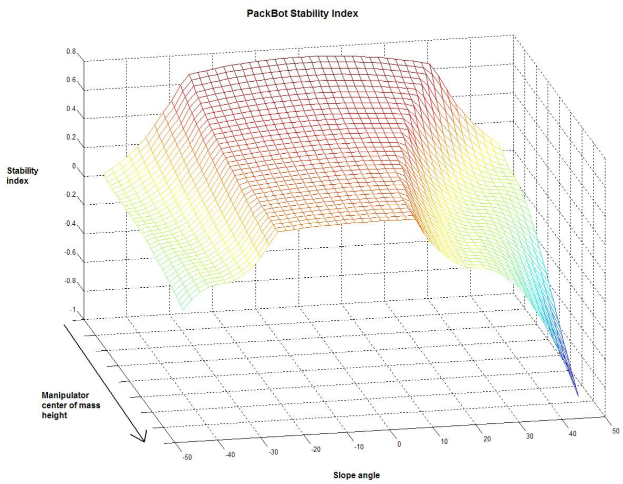

Fig. 7. Manipulator center of mass height effects on tip over stability

Figure 8 shows the effect of the flippers on the tip over stability. The flippers are modelled rotating through a full 360^o motion with the manipulator stowed. During the flipper up range of motion, the stability index is constant through any particular slope angle. As the slope angle moves away from 0^o, the stability index in the flipper up range of motion decreases. During the flipper down phase, when the flippers are in contact with the ground ,there is a high stability region with two distinct boundaries. As the slope angle moves away from 0^o, the size of the stable region decreases. When the PackBot is facing upslope stablity decreases when the flippers are in contact with the ground. When the PackBot is facing downslope stablity increases for a certain range of the flipper angle when the flippers are in contact with the ground. Thus when facing downslope, lowering the flippers would increase the stability.

V. Conclusion

The model of a tracked mobile manipulator detailing the pose of the manipulator and flippers has been presented in this paper. Tip over stability analysis of the system reveals that the pose manipulator and flippers of tracked mobile manipulators have a large impact on the tip over stability of the system. The pose of the manipulator and flippers can thus be used to prevent tip over of the mobile manipulator. When the PackBot

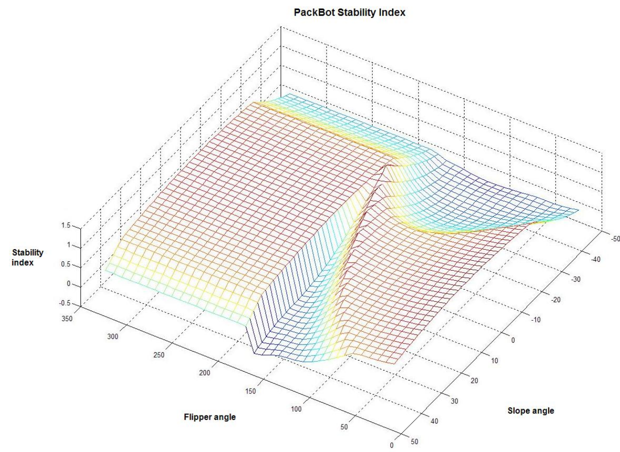

Fig. 8. Flipper effects on tip over stability

is facing downslope, the flippers should be lowered to increase stability. As the magnitude of the slope angle increases, the center of mass height of the manipulator should be kept low. For slopes close to 0^o the manipulator angle should be kept close to 25^o and for slopes below 0^o the manipulator angle should be kept close to 200^o.

References

[1] Q. Huang, S. Sugano, and I. Kato, "Stability control for a mobile manipulator using a potential method," in *Proceedings of the the IEEE/RSJ/GI International Conference on Intelligent Robots and Systems,* 1994, vol. 2, pp. 839-846.

[2] J. Kim, W. K. Chung, Y. Youm, and B. H. Lee, "Real-time zmp compensation method using null motion for mobile manipulators," in *Proceedings of the the IEEE International Conference on Robotics and Automation,* 2002

[3] E. Papadopoulos and D. Rey, "A new measure of tipover stability margin for mobile manipulators," in *Proceedings of the IEEE International Conference on Robotics and Automation,* 1996, vol. 4, pp. 3111-3116.

[4] D. A. Rey and E. G. Papadopolous, "On-line automatic tipover prevention for mobile manipulators," in *Proceedings of the the IEEE/RSJ International Conference on Intelligent Robots and Systems,* 1997, September

[5] E. Papadopoulos and D. Rey, "The Force-Angle Measure of Tipover Stability Margin for Mobile Manipulators," Vehicle System Dynamics, 2000, 33, pp. 29-48.

[6] S. A. A. Moosavian and K. Alipour, "Stability evaluation of mobile robotic systems using moment-height measure," in *Proceedings of the the IEEE International Conference on Robotics, Automation, and Mechatronics,* 2006, June, pp. 97-102.

[7] S. A. Moosavian and K. Alipour, "Moment-height tip-over measure for stability analysis of mobile robotic systems," in *Proceedings of the the IEEE/RSJ International Conference on Intelligent Robots and Systems,* 2006, October, pp. 5546-5551.

[8] P. R. Roan, A. Burmeister, A. Rahimi, K. Holz, and D. Hooper, "Real-World Validation of Three Tipover Algorithms for Mobile Robots," in *Proceedings of the the IEEE International Conference on Robotics and Automation,* 2010, May, pp. 4431-4436.

[9] Q. Huang and S. Sugano, "Manipulator Motion Planning for Stabilizing a Mobile-Manipulator,"

[10] Q. Huang, K Tanie, and S. Sugano, "Stability Compensation of a Mobile Manipulator by Manipulator Motion: Feasibility and Planning,"

[11] Sciavicco, L., Siciliano, B., *Modelling and Control of Robot Manipulators,* London: Springer-Verlag, 2005.

[12] iRobot, "Ground Robots - 510 PackBot", http://www.irobot.com/gi/ground/510_PackBot/for_EOD_Technicians